First Ring Formation by Radical Addition of Propargyl to But-1-ene-3-yne in Combustion. Theoretical Study of the C7H7 Radical System.

UNIVERSITÀ DEGLI STUDI DI TORINO

First Ring Formation by Radical Addition of Propargyl to But-1-ene-3-yne in Combustion. Theoretical Study of the C_7H_7 Radical System.

Daniela Trogolo,[1] Andrea Maranzana,* Giovanni Ghigo, and Glauco Tonachini*

Dipartimento di Chimica, Università di Torino, Corso Massimo D'Azeglio 48, I-10125 Torino, Italy

Abstract. Combustive formation of a first carbon ring is an important step in the growth of polycyclic aromatic hydrocarbons (PAHs) and soot platelets. Propargyl radical addition to but-1-ene-3-yne (vinylacetylene) can start off this process, possibly forming 5-, 6-, and 7-membered rings. A variety of partially intertwined reaction pathways results from density functional theory (DFT), which indicates three C_7H_7 radicals, benzyl, tropyl, and vinylcyclopentadienyl, as particularly stable. DFT energetics forms a basis for a subsequent RRKM study at different combustion pressures and temperatures (P=30-0.01 atm; T=1200-2400 K). RRKM indicates (Figure 4) open-chain structures and 5-rings as the most important products. Open-chain structures, whose main contributors are the initial adducts, are favored by lower T and higher P, while 5-rings are favored, by contrast, by higher T and lower P. The main feature is that the declining yield in open-chain structures with rising T almost mirrors, at all pressures, the growth with T exhibited by 5-rings (main contributor: fulvenallene). Thus the two yield lines for open chains and 5-rings cross at some T, and their crossing moves towards lower T values as lower P values are considered (plots 4a to 4d). Since the T dependence of the yields (slope of the lines) is more pronounced in the T range close to the line crossing, it also becomes less pronounced at the lowest P values considered, since the crossing region falls at very low T values. Another constant trait is that 6-rings (mainly benzyl radical) are the third contributor, though they are present at most with a modest maximum yield of 2.4–2.7% in a T range which moves towards lower T as P is reduced.

Keywords: PAH formation; first C-ring; propargyl; but-1-ene-3-yne; vinylacetylene

Running Title: Ring closures in propargyl + but-1-ene-3-yne

***Corresponding authors:**

e-mail: glauco.tonachini@unito.it - phone: ++39-011-6707648 - fax: ++39-011-2367648
e-mail: andrea.maranzana@unito.it - phone: ++39-011-6707637 - fax: ++39-011-2367637

[1] present address: Environmental Chemistry Modeling Laboratory, Swiss Federal Institute of Technology at Lausanne (EPFL), 1015 Lausanne, Switzerland.

1. Introduction

The impact of carbonaceous particulate[1,2] and polycyclic aromatic hydrocarbons (PAHs) on the environment in general,[3,4] and human health in particular, is significant, because C-particulate gives a major contribution to the overall mass of atmospheric aerosol, and PAHs exhibit an ubiquitous presence. PAHs and PAH cations, PAH clusters, and amorphous carbon clusters are also of astrophysical interest, since they have been identified (to some extent tentatively) out of the terrestrial environment, namely in planetary atmospheres,[5,6] in the envelopes of carbon-rich stars,[7,8,9] or in the interstellar medium,[10] hence under a large variety of pressure and temperature conditions. This interest has recently prompted, for instance, combined experimental and theoretical work on cosmic-ray-mediated benzene formation.[11] On the other hand, graphene sheets, graphene nanoribbons, and synthetic ways to very large PAH systems[12,13,14,15] have in recent years been deemed promising from a technological point of view,[16] to build capacitors,[17,18] sensors,[19,20] transistors and circuits in general,[21] and so forth.

Soot and PAHs share the same nature and origin,[22,23,24,25,26,27] and the latter are often considered as soot precursors, though other opinions have been set forth.[28] Homann, for instance, put forward[29] that the reactions leading to PAHs could also bring about the formation of more irregular structures, called "aromers" (see ref. 29, pp 2448-2450), starting from associations between PAHs and subsequent H_2 losses. These intermediate structures could grow as cages with a higher or lower H content, and get some curvature. Curvature can be induced in different ways by non-hexagonal carbon rings, such as 5-membered rings (5-ring for short in the following) or 7-rings. Aromers could be seen as candidate precursors of fullerenes and soot, depending on temperature and the relative abundance of small growth components, as HCCH.

Since the growth mechanisms and association modes of PAHs and soot platelets are not completely clarified, we have recently attempted to give some contribution, possibly complementary to the experiment. Namely, we have studied theoretically the growth of an aromatic system adsorbed on a model soot platelet[30] and the feasibility of van der Waals associations (stacking) and σ bond formation between PAH-like molecules as a function of temperature (i.e. during or after a combustion process).[31,32] Now, the formation of the very first (possibly aromatic) ring molecule from small aliphatics, which is our present focus, has been often seen as the rate-determining step of soot growth, and appears in any case particularly interesting.[33,34] Formation of aromatics and soot particles, in particular the issue of first ring formation, were reviewed and discussed by Richter and Howard in 2000,[33] and by Frenklach in 2002.[34] Hence we will not deal at length with earlier mechanistic proposals. Among these, Bittner

and Howard[35] suggested benzene formation via the butadienyl (CH_2=CH–CH=CH$^\bullet$ or CH_2=CH–C$^\bullet$=CH_2) plus ethyne reaction. This idea was partly supported by an experiment in which butadienyl formation in a 1,3-butadiene flame was observed.[36] Subsequently, similar mechanisms were also proposed by the same groups,[37,38,39,40] such as, for instance, the sequence triggered by vinyl (CH_2=CH$^\bullet$) addition to (a) ethyne [$C_2H_3^\bullet$ + C_2H_2 → n-$C_4H_5^\bullet$; n-$C_4H_5^\bullet$ + C_2H_2 → n-$C_6H_7^\bullet$; n-C_6H_7 → C_6H_6 + H$^\bullet$] or (b) to but-1-ene-3-yne (vinylacetylene, CH_2=CH–C≡CH), or also (c) [CH_2=C$^\bullet$–C≡CH + C_2H_2 → $C_6H_5^\bullet$] the latter being however deemed unlikely in a later study.[41,42] Some flame studies indicated that the recombination of the propargyl radicals $(H_2CCCH)^\bullet$ can be the dominant pathway to first ring formation[40,43,44] (in particular Stein and coworkers pointed out that recombination products of propargyl radicals in flames irreversibly generates benzene and fulvene).[45] Furthermore, theoretical studies by Miller and Melius[41] and, more recently, by Miller and Klippenstein[46] showed that the addition of two propargyl radicals[47,48,49] accounts satisfactorily for several experimental results concerning either benzene or phenyl radical formation.

First ring formation has also been the subject of more recent experimental and theoretical investigations of different ring closure processes, such as those of Hansen and coworkers on the formation of several 5- and 7-membered rings in a cyclopentene flame,[50,51,52,53] or those by Mebel, Kislov, and Kaiser on phenyl radical formation through C_2 + buta-1,3-diene (C_4H_6) reactions,[54] or on the formation of slightly larger systems, such as (dihydro) naphthalene,[55,56,57] or indene[58], and pentalene.[59] Similarly, that, on indene formation, by Vereecken and coworkers.[60] Other reactions investigated recently by Cavallotti, Derudi, and Rota,[61] and by da Silva, Cole, and Bozzelli,[62,63] bear a strict relationship with that studied in the present paper. They take place on the very same $C_7H_7^\bullet$ energy hypersurface that will be explored in the present study, and are: cyclopentadienyl + ethyne, fulvenallene + H, and 1-ethynylcyclopenta-diene + H. Our title reaction will rather obviously share a fairly extended number of intermediates with them, and they will consequently be recalled in Section 3. Other studies have considered in general the mechanism of PAH growth.[64] Along this line, we have already examined[65] the first growth steps of aromatic systems through the ring closure-radical breeding polyyne-based mechanism proposed by Krestinin[66,67,68] (polyynes had already been considered at an earlier time by Homann and Wagner[69]).

In the present paper we explore, under combustion conditions, the possible formation of 5-, 6-, or 7-membered ring intermediates, having energies close or below that of the reactants, which could be involved in subsequent PAH or soot platelet growth processes. The reacting $C_7H_7^\bullet$ system examined is defined by the radical addition of propargyl to but-1-ene-3-yne (Chart 1; the two resonance structures illustrate qualitatively that π–electron delocalization is present to some

degree). If propargyl was considered originally in the mentioned studies[41,46] as a species capable in itself of generating benzene through self-addition, other reactions, e.g. between propargyl and alkynes, are likely to play an important role in the hydrocarbon growth process. We can mention for instance that the kinetics of the related reaction between the propargyl radical and ethyne has been investigated both experimentally[70] and theoretically.[71] The reaction between propargyl and butadiyne has also been investigated theoretically.[72,73] To our knowledge, no gas-phase experimental study involving propargyl and alkenes has been carried out.[74,75,76]

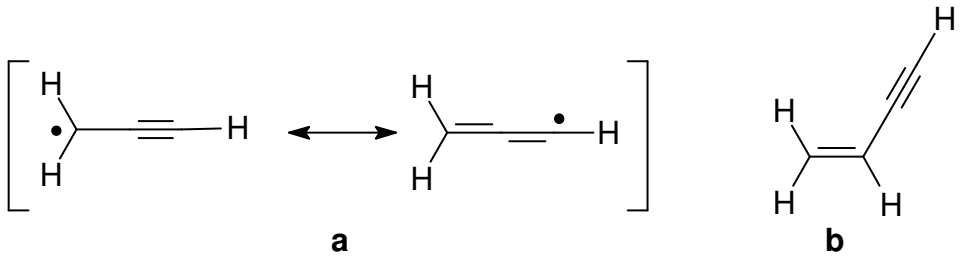

a **b**

Chart 1.

Both the propargyl radical and but-1-ene-3-yne have been recently reported to reach not negligible molar fractions x, in the ranges x = 2–3 x10^{-3} and 2x10^{-4} – 2x10^{-3}, respectively.[77] They were detected in the oxidation zone of premixed ethyne,[78] benzene,[79] toluene,[80] or gasoline[81] flames. Similarly, a propargyl molar fraction up to x = 1 x 10^{-3} or 2.4 x 10^{-4} was detected either in dimethyl ether/propene and ethanol/propene[82] or benzene/oxygen/argon[83] low-pressure flames.

2. Theoretical Method

All stationary points on the energy hypersurface, *i.e.* minima and first order saddle points, corresponding to transition structures (TS), were determined by gradient procedures[84,85,86,87,88] within the Density Functional Theory (DFT),[89] and making use of the M06-2X[90,91,92,93] functional. The cc-pV*TZ* basis set[94] was used throughout in the DFT optimizations. The nature of the critical points was checked by vibrational analysis, which allowed us also the thermochemistry assessment. The optimizations were followed by cc-pV*QZ*[95] single-point energy computations, to finally obtain M06-2X/CBS (complete basis set) energy estimates through the extrapolation formula put forward by Halkier et al.:[96] $E_{X,Y} = (E_X X^3 - E_Y Y^3)/(X^3 - Y^3)$. The energy estimate $E_{X,Y}$ exploits the energies obtained with the two basis sets cc-pVXZ or cc-pVYZ: E_X and E_Y, respectively. In this study, X=3 and Y=4, and the two-point formula is thus simply used as: $E_{3,4} = (E_3\, 3^3 - E_4\, 4^3)/(3^3 - 4^3)$. The cc-pV*TZ* thermochemical corrections gave estimates of the zero point vibrational energy, by which the relative energies were corrected to obtain ΔE_{ZPVE} [= $\Delta(E$ + ZPVE)] values. These ΔE_{ZPE} values at DFT(M06-2X)/CBS are reported throughout in the text. The thermochemistry was assessed in all cases at temperatures typical of combustion (T in Kelvin degrees, energetics in

kcal mol^{-1}). Geometry optimizations and thermochemistry calculations were carried out by using the GAUSSIAN 09 system of programs.[97]

We are aware that further comparison of DFT energetics with that defined by other more demanding methods, such as coupled cluster or quadratic CI, could be attractive, but the extended number of structures involved in this seven-C atom reaction makes this level of study not affordable. In the Appendix, a validation of the computational level adopted in this study is presented, hoping it might help in estimating the accuracy of the method adopted and the degree of confidence that can reverberate to the RRKM analysis that follows.

The Rice Ramsperger Kassel Marcus (RRKM) theory,[98,99] fundamental development of the unimolecular kinetic theory elaborated by Lindemann[100] and Hinshelwood,[101] was then used to obtain the distribution of the reaction products. In order to obtain these distributions as functions of time, RRKM and Master Equation calculations (RRKM/ME) were carried out by using the Multiwell program suite.[102,103,104] It allows to calculate sum and densities of states, then obtains micro-canonical rate constants according to RRKM theory, and finally solves the master equation. Corrections for quantum tunneling were included for all hydrogen transfer reactions (not H dissociations) by incorporating the corrections for one-dimensional unsymmetrical Eckart barriers.[105] Internal rotations were treated as unsymmetrical hindered rotations, by using the *lamm* program, supplied with MultiWell. MultiWell stores densities and sums of states in double arrays: the lower part of the array consisted of 999 array elements which ranged in energy from 0 to 9990 cm^{-1}. The higher energy part of the double array consisted of 1001 elements ranging in energy from 0 to 150000 cm^{-1} with an energy spacing of 150 cm^{-1}. The Lennard-Jones parameters necessary for the collision frequency calculations were assumed to be the same for all the structures, were: σ = 5.92 Å, and ε/k_B = 410 K. Energy transfer was treated by assuming the exponential-down model for collision step-size distributions (E_{down} = 2000 cm^{-1}, independent from the temperature). E_{down} and the Lennard-Jones parameters are the same used by da Silva et al.[63,106] to study the benzyl decomposition reaction. Rate constants were calculated in the range 1200-2400 K. In the present work, the number of stochastic trials was set to 10^7, for 200 collisions.[107] Simulations were carried out for combustion temperatures, at different pressures (of N_2 buffer gas), namely at P = 0.01, 0.1, 1, and 30 atm, to simulate combustions under low,[83,108,109,110,111,112,113,114] normal, and high[115] pressure conditions. Multiwell code uses stochastic methods to solve the energy-grained master equation, but does not calculate the rate coefficients *k*(T,P). In order to obtain approximated *k*(T,P), we used the Post-Processing in Multiwell (PPM) program, developed by Pinches and da Silva,[116] to separate the contributions of chemically and thermally activated reactions. Rate constants were calculated by multiplying the

high-pressure limit rate constant for the propargyl + but-1-ene-3-yne reaction, by the chemically activated yields for all the channels. The rate constants calculated for each of the four entrance channels were summed to obtain the total rate constants.

3. Results and discussion

3.1 Potential energy surface

Initial steps. Eight entrance channels are considered. They correspond to the addition of each of the external carbons of the propargyl radical (Chart 1a) to the four unique positions of but-1-ene-3-yne (Chart 1b). However, the four propargyl additions to the external carbons of but-1-ene-3-yne (Table 1: entries 1-4) have lower energy barriers compared to the additions to its internal carbons (Table 1: entries 5-8).

Table 1. Entrance channels: ΔE_{ZPVE} (kcal mol^{-1}) barriers for the initial radical additions[a]

Channel	ΔE_{ZPE}	Channel	ΔE_{ZPE}
1	7.42	**5**	13.46
2	9.35	**6**	15.37
3	9.84	**7**	14.74
4	10.72	**8**	14.88

This feature reflects the stability of the initial open-chain adducts, of which only the first four present delocalization of the unpaired electron. Making reference to the reagents, they are located at -21.3 (1), -15.5 (2), -23.5 (3), -26.7 (4) kcal mol^{-1}, respectively. Scheme 1 shows the reaction pathways that start from these lower-barrier additions. Through them, the system evolves by intramolecular radical additions and subsequent cyclizations, then ring openings and hydrogen shifts. Because of some cyclizations and ring openings, also the initial adducts 5-8 can form. Boxes highlight all initial adducts 1-8 (1 and 7: center of Scheme 1; 3 and 5: top; 6, 4, and 2: left, proceding towards the bottom; 8: bottom). Intermediate ring products, which can be in principle of particular interest because of the low energy, are vinylcyclopentadienyl, tropyl, and benzyl radicals. These are highlighted instead by dashed boxes. The structures are not connected by arrows, but only by segments, with the declared purpose of not specifying preferred directions of flow along the pathways. Only irreversible steps, through which lower weight-intermediates are obtained via fragmentation (loss of H, loss of HC≡CH), are indicated by arrows. It must be stressed in this regard that the RRKM results can modify the picture provided by the energetics to a significant extent.

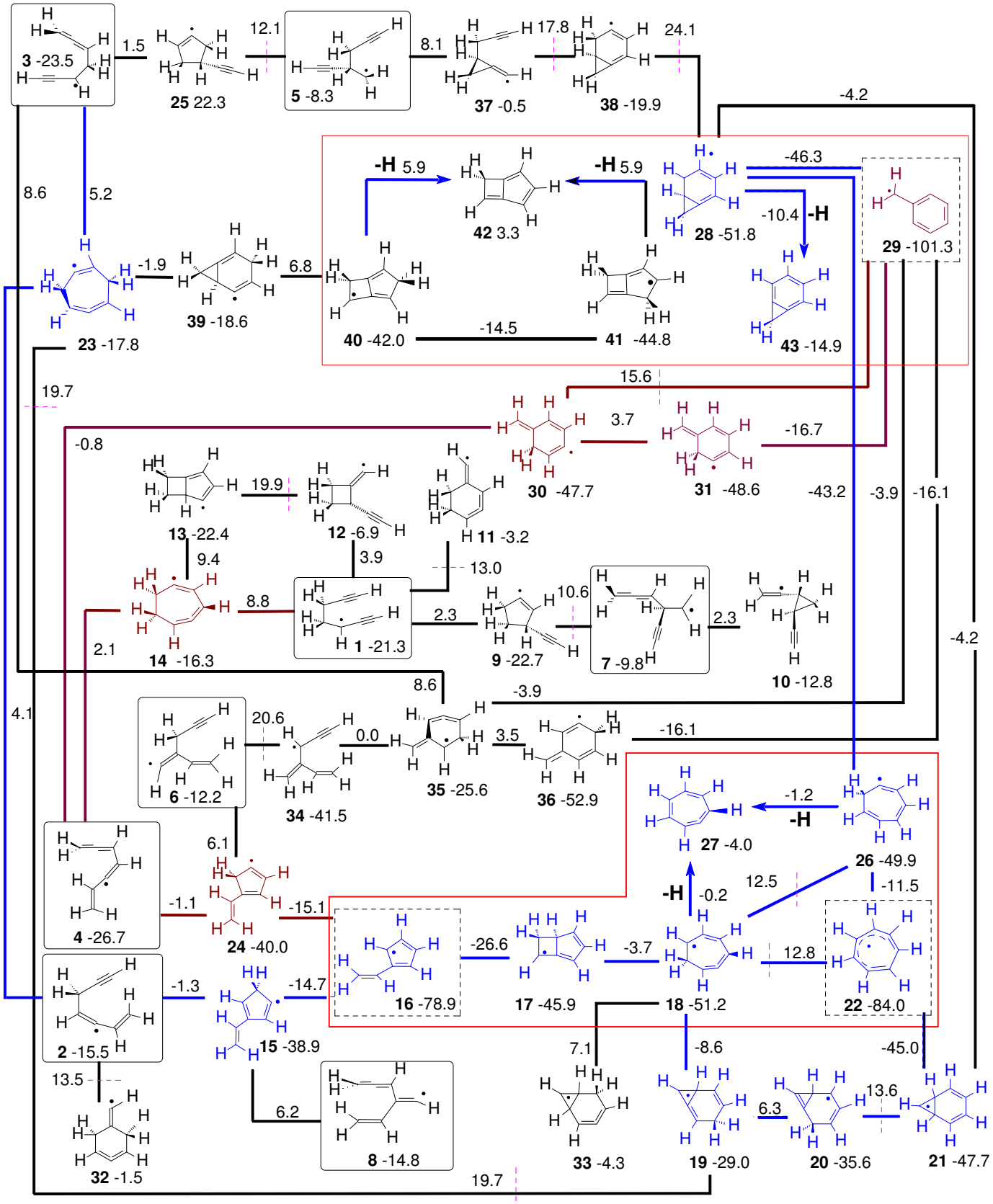

Scheme 1. Initial pathways toward 5-, 6-, and 7-ring intermediate structures. Initial open-chain adducts 1-8 are enclosed in gray boxes. Dashed gray boxes draw attention to $C_7H_7^{\bullet}$ intermediates which appear prominent because of low ΔE_{ZPE} values (16, 22, 29). Some intermediates are obtained through irreversible fragmentation steps (**- H** and arrows). Red contours encompass structures that will be found also in Scheme 2. Structure color code (blue, dark red) as for structures and energy profiles of Figures 1, 2, and 3.

The apparently most promising reaction steps, chosen on the basis of the ΔE_{ZPE} values (barriers lower than 20 kcal mol^{-1}), will be commented in the following relying on the color code present in Scheme 1, and consistently adopted in Figures 1–3. Due to some intricacies in the network, the numeric labels mentioned will be often not sequential. Further reaction channels departing from some intermediates are described in Scheme 2. It can be observed that the initial adducts 1-4 are interconnected through steps which involve fairly moderate height barriers, ranging from 2.1 to 8.8 kcal mol^{-1} (Figure 1). The adduct 1 is connected to the adduct 4 through the 7-ring 14 (ring closure, ring opening: mid-left of Scheme 1).

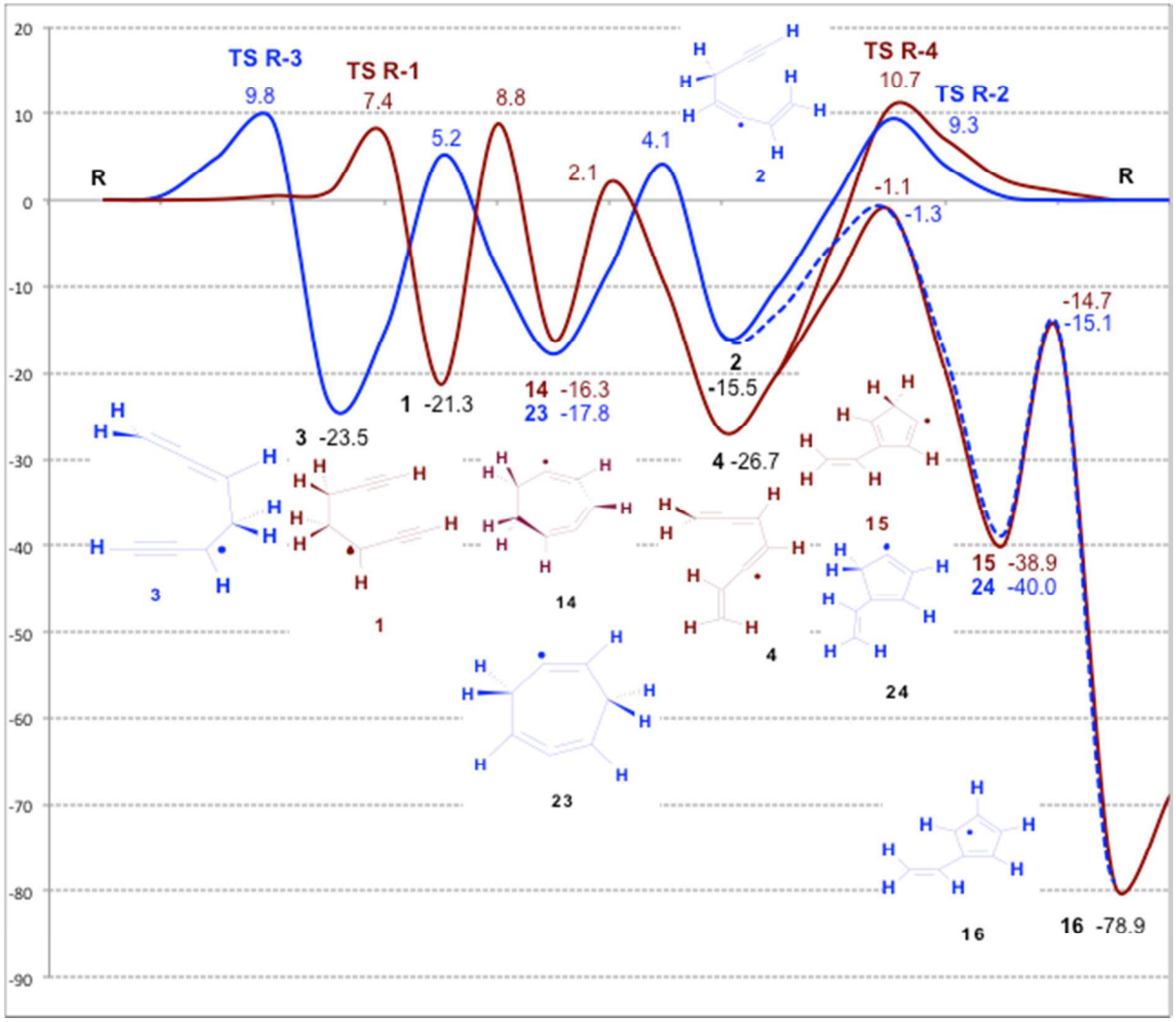

Figure 1. Interconversion pathways of the initial adducts, and steps toward 5-rings. The linear structures 2 and 3, blue line, as well as 1 and 4, dark red line, can form directly from addition of the reactants R (left and right). Structure 2 is connected to 3 through 23 ; similarly, 1 and 4 through 14 (compare Scheme 1). All these converge on the 5-ring structure 16 through 15 or 24.

Similarly, the adduct 3 is connected to the adduct 2 through the 7-ring 23 (center of Figure 1, blue line, and top-left to bottom-left in Scheme 1). From 2 and 4, however attained, the very stable (-79 kcal mol^{-1}) vinyl-substituted cyclopentadienyl radical intermediate 16 can form in two steps (Figure 1, right). In 2, a first cyclization, through a radical attack on the terminal carbon of the triple bond, produces the vinyl-substituted 5-ring 15. From 4, a radical attack on the terminal carbon of its allenic part gives the 5-ring 24, an isomer of 15. Then, in both cases, a 1,2 H shift leads down to 16 (bottom-left of Scheme 1, then to the right). A further connection between 5- and 6 rings, and possibly also 7-rings is described in Figure 2. Finally, different steps from 1 and 4, or from 22, that lead to the 6-ring benzyl radical are displayed in Figure 3. These plots are introduced because they connect the initial adducts to the very stable intermediates 16 and 22 (bottom of Scheme 1), and 29 (top right of Scheme 1).

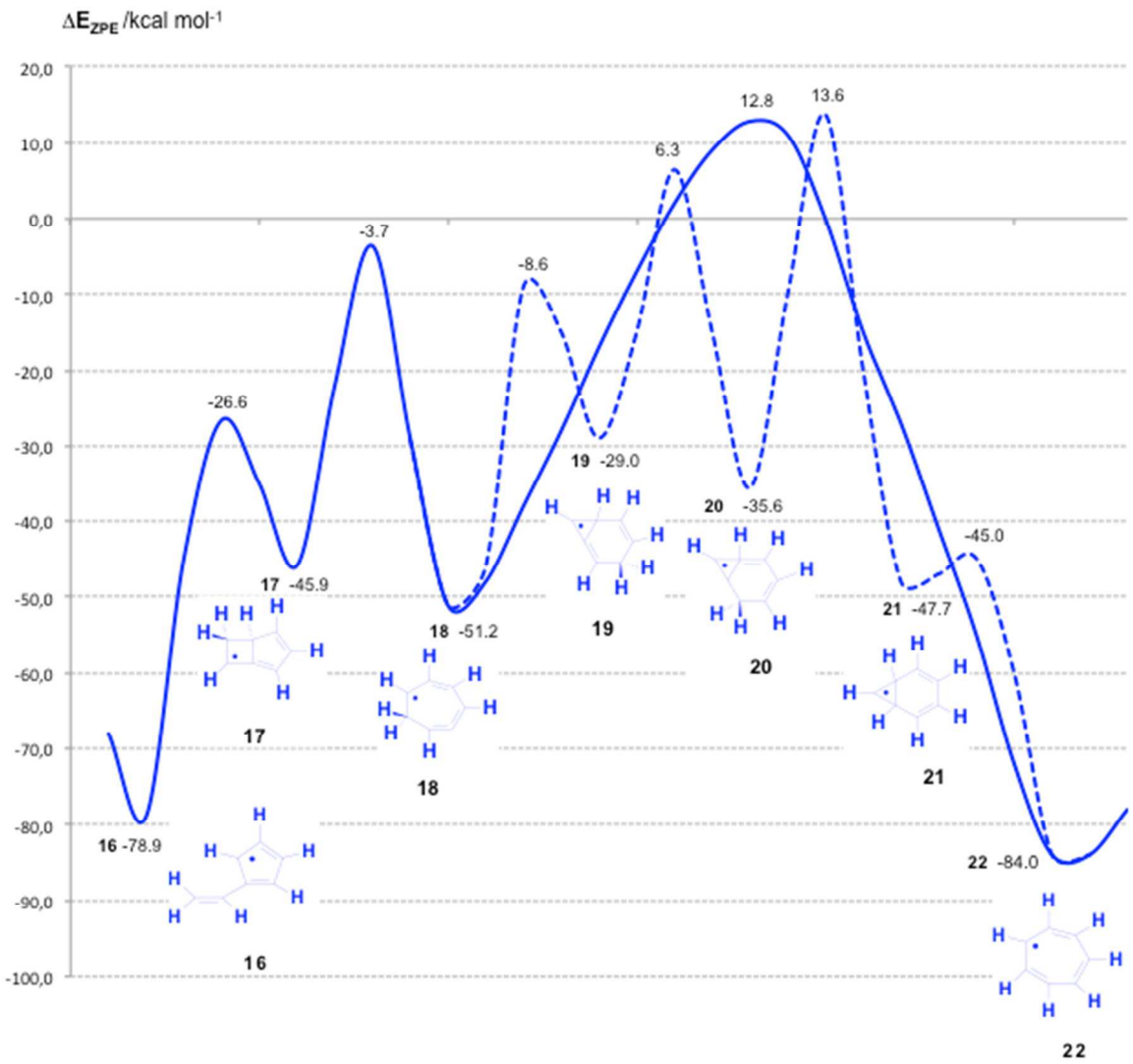

Figure 2. Steps connecting 5-rings to 6- and 7-rings.

A 4-ring closure in 16 gives 17, and is followed by ring size extension to the allenic 7-ring 18. A ring closure to the fused bicyclic intermediate 19 might be followed the somewhat unpromising sequence of two 1,2 H shifts, to give its isomers 20 and 21. From the latter, through a cleavage of the fusion CC bond, the system might plummet down to -84 kcal mol^{-1}, in correspondence of the cycloheptatrienyl (tropyl) radical 22 (Figure 2 and lower red box in Scheme 1).[117,118,119,120] Another variant directly connects 18 to 22. The barriers involved is high enough to limit the formation of 22, if the system were efficiently thermalized.

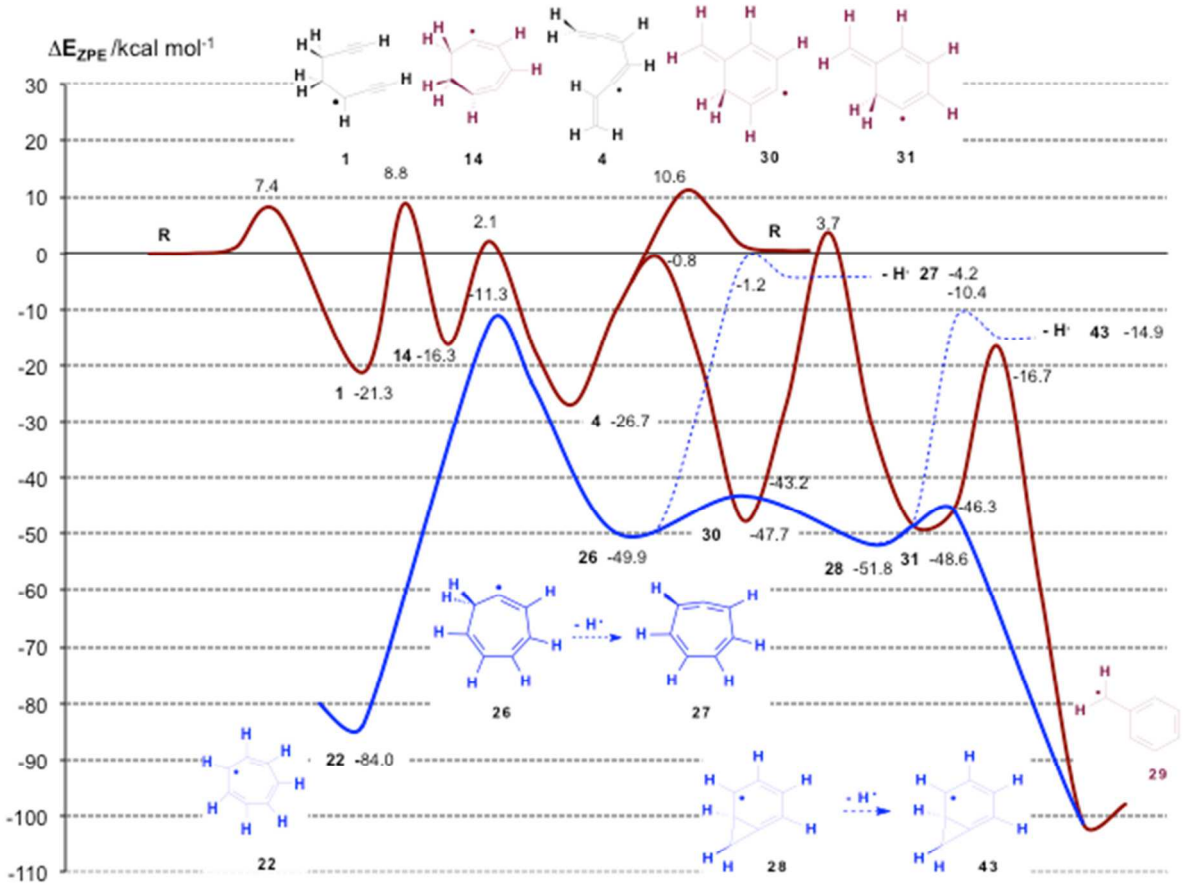

Figure 3. Steps that might in principle lead to the 6-ring benzyl radical 29. Dark red profile: see dark red pathway in Scheme 1. The linear structures 1 and 4 can form directly from addition of the reactants R (black structures). The blue profile can be seen as a continuation of Figure 2. Thin dashed lines refer to H losses.

Another pathway (top of Scheme 1) could start from the initial adducts 3 or 5 (connected through 25, a cyclization product). Two cyclizations lead from 5 to 37 and 38, with barriers above the reactants reference level. Then only a difficult H shift connects it with 28, a necessary step toward the very stable benzyl radical 29 (-101 kcal mol^{-1}). Thus, this pathway can hardly be seen as viable. Another pathway, which looks more promising to get benzyl, starts from the initial adducts 1 or 4 (connected through 14). See dark red lines in Figure 3 and center of Scheme 1. A cyclization in 4 gives 30, then one H shift leads to 31, and a second one to 29, all steps being

below the reference level. However, we can notice again that, in case the system were effectively thermalized, the highest barriers involved could be demanding enough to make the formation of the benzyl radical difficult.

Also tropyl 22 is connected to 28, through 26, hence to 29 too. We can note that 28 can lose one hydrogen atom and give 43, just as 18 an 22 in producing 27 (rightmost part of Scheme 1). These H losses present higher barriers than some competing steps (as 26-28, or 28-29), but are irreversible and entropy-favored. With time, they might be able to "pump away" from the C_7H_7 system.

The cyclic intermediates enclosed in red contours in Scheme 1, some of which are quite low in energy, present connections with further pathways (Scheme 2). They too are to some extent intertwined. Most of the species involved contain 5-membered rings. They had mandatorily to be considered to carry out the RRKM/ME study that follows, though several of these structures have already been described by other researchers within studies on systems different by the present one. For this reason they will be no commented at length. In fact, different papers have appeared in recent years in which the decomposition of benzyl derivatives was examined experimentally[121] as well as theoretically[61,63,63,106] (benzyl radical is encountered as structure 29 in the present study). In studies by Cavallotti, Derudi, and Rota,[62] and by da Silva, Cole, and Bozzelli,[63,63] the importance of the fulvenallene intermediate (here system 62) was stressed. Fulvenallene is a product of H loss.

Some of the intermediates in Scheme 2 appear noticeable because of their stability, though none attains the stability of those highlighted in Scheme 1. Other are conspicuous because they form irreversibly upon fragmentation. However, RRKM/ME results (for which all the pathways shown in the schemes are necessary) can modify the picture offered by the energetics alone to a significant extent. These aspects we will discussed presently in the next section.

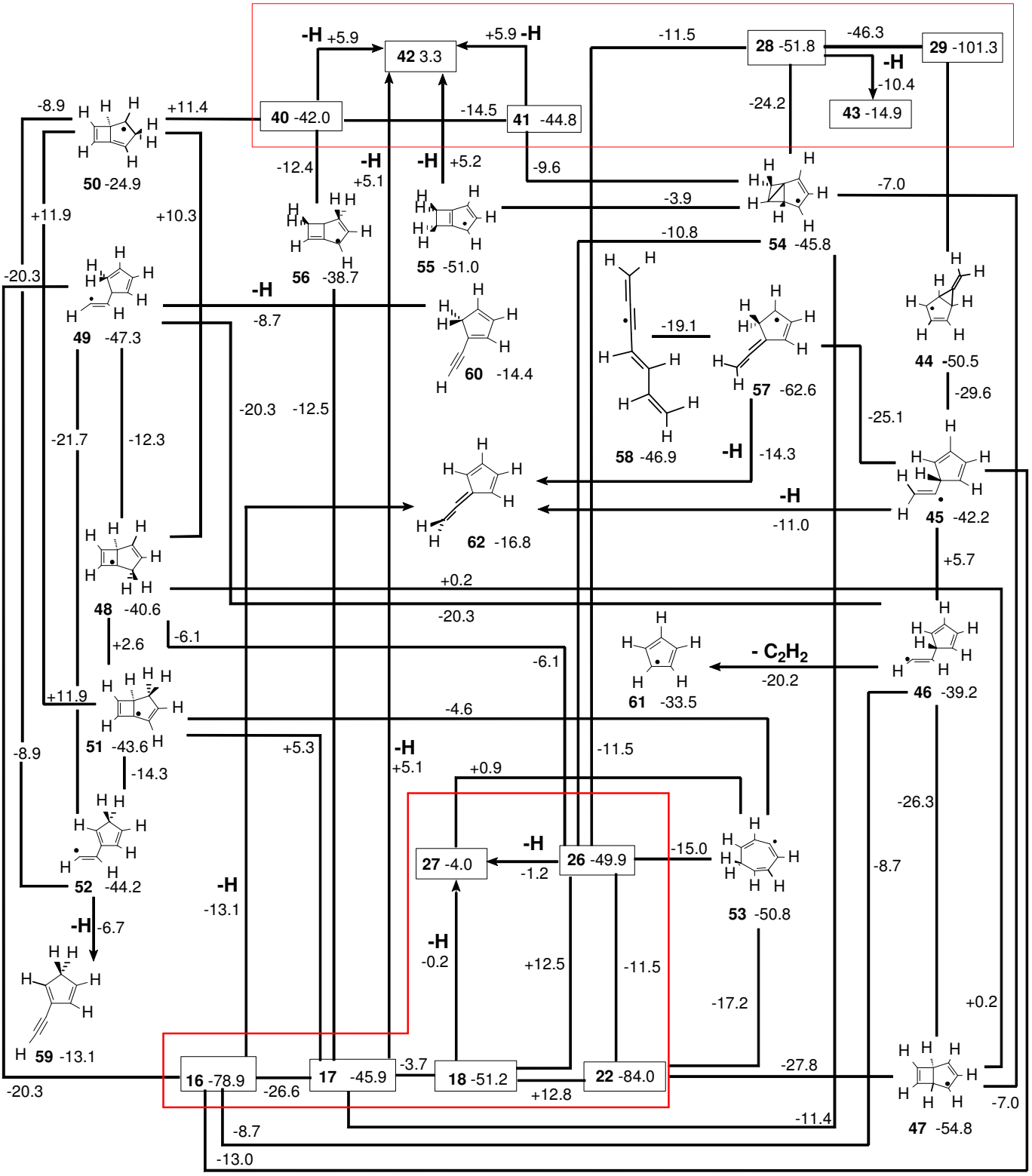

Scheme 2. Further pathways mainly toward other 5-ring structures. Red contours encompass boxed structures which were already found in Scheme 1. Arrows indicate irreversible steps (**- H**, **- C_2H_2**). When resonance occurs, only one structure is shown.

3.2 Master equation simulations.

RRKM-ME simulations show that the initial adducts 1-4 give back-reaction to the original reactants to a significant extent. It more easily occurs at high temperature and low pressure. Since this effect is not observable in the yield experiments, the computational results reported in this paper have been corrected for it: the *net product reaction yields* reported in Figure 4 exclude the redissociation to the initial products. For each of the four entrance channels (Table 1: entries 1-4), separate simulations were carried out, then the total yields were calculated by weight-averaging[122] the individual channels. In order to computationally access a temperature range sufficiently wide to be of interest for combustion or pyrolysis, the kinetic simulations were carried out in the range 1200 K $\leq$ T $\leq$ 2400 K. Since the results vary not only as a function of T but also of P, we have studied the net product reaction yields at four pressure values: P = 30, 1, 0.1, and 0.01 atm. On the high pressure side, the data plotted in Figure 4 could be related to internal combustion engine chemistry,[115] while the low pressure data can be seen as pertinent to the oftentimes used low-pressure flames.[108]

At P = 30 atm (Figure 4a), the importance of 5-rings as a class grows from 1-2% at T = 1200 K over the entire T range studied, rising steeply to 38% of the total product yield at T = 2100 K, then up to 70% at T = 2400 K. This behavior is mirrored by the yield of open-chain products (represented mainly by the initial adducts), which dominate at T = 1200-1800 K (98-91% of the total product yield) but falls off significantly at the highest temperatures. These two yield curves present a crossing point around T = 2200 K. Their yield is still 61% at T = 2100 K, but plunges down to 27% at T = 2400 K. Next come 6-rings, which form only in modest quantities: their yield grows almost linearly with T, just above 2% at 2100 K, up to 2.7% at T = 2400 K.

At P = 1 atm (Figure 4b), open-chain structures persist as the most important contribution only below T = 1500 K (89 to 49%), since they decline severely as T rises. 5-Rings represent, at the lowest T value, only less than 11%, but their yield rises with T. At T $\approx$ 1500 K, open-chain products and 5-rings represent 49% of the total product yield each (thus the crossing of the two yield curves has moved, comparing with P = 30 atm, toward a lower temperature). Then, 5-rings begin to dominate for T > 1500 K (78 to 93% beyond 1800 K). At P = 1 atm, the declining yield in open-chain structures almost mirrors, as for P = 30 atm, the growing trend exhibited by 5-rings, while both curves seem to move to the left, towards lower temperatures, as pressure is lowered. The yield in 6-rings is 2.5% within the approximate T range 1600-1900 K, where it shows a quite flat maximum zone.

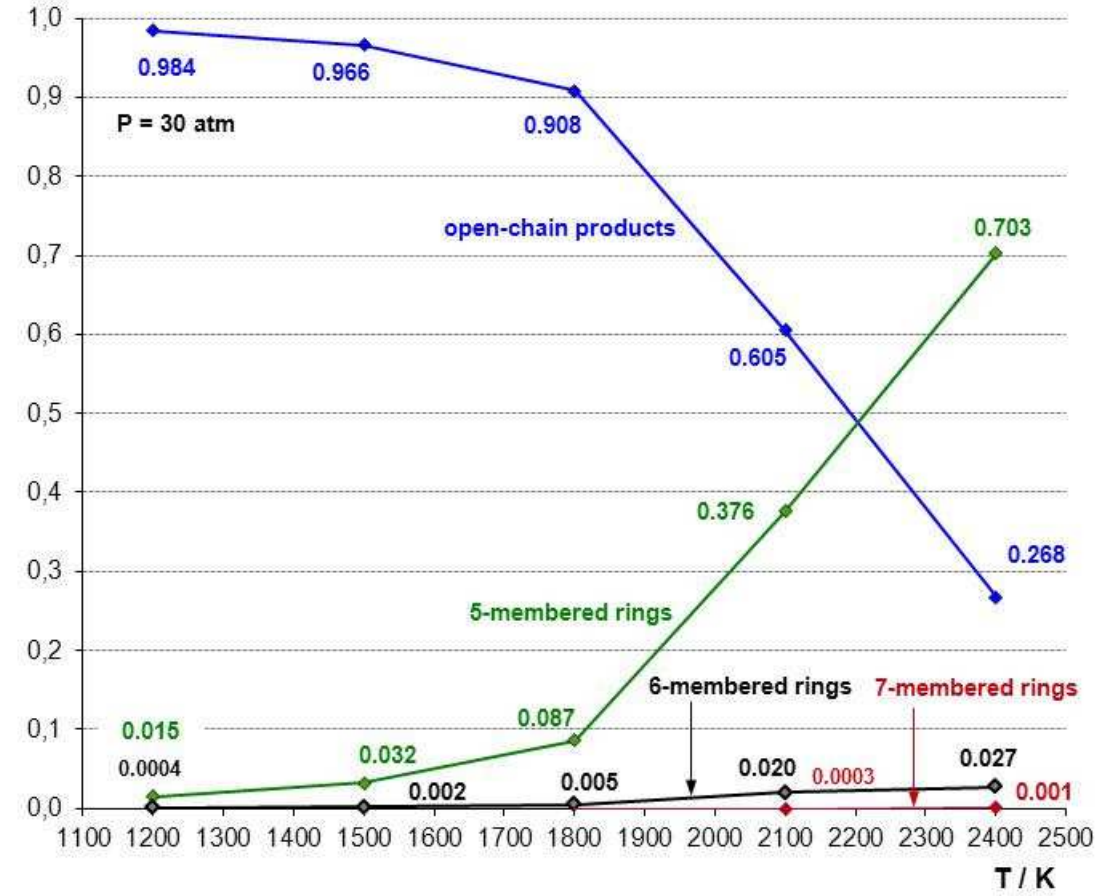
P = 30 atm
open-chain products
5-membered rings
6-membered rings
7-membered rings
0.984
0.966
0.908
0.605
0.268
0.703
0.376
0.087
0.032
0.015
0.0004
0.002
0.005
0.020
0.0003
0.027
0.001
T / K

a

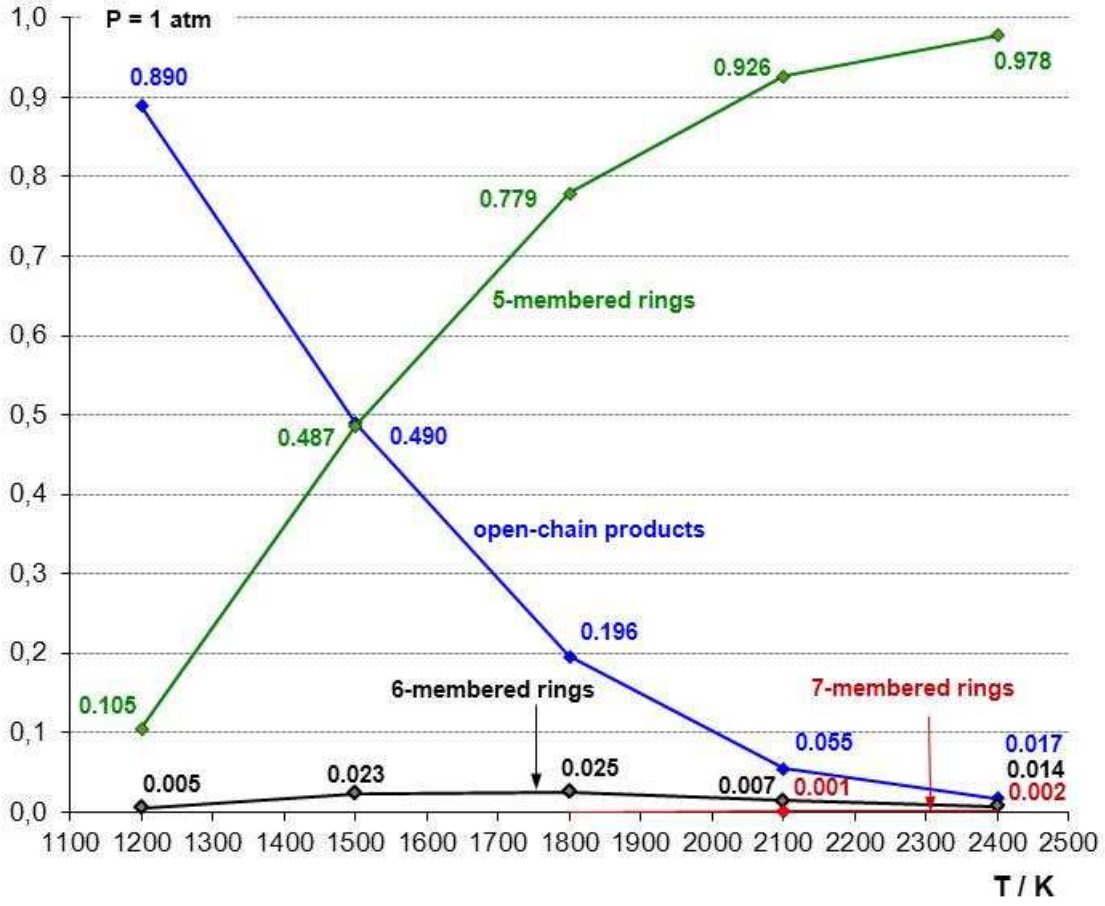
P = 1 atm
open-chain products
5-membered rings
6-membered rings
7-membered rings
0.890
0.196
0.055
0.017
0.926
0.978
0.779
0.487
0.490
0.105
0.005
0.023
0.025
0.007
0.001
0.014
0.002
T / K

b

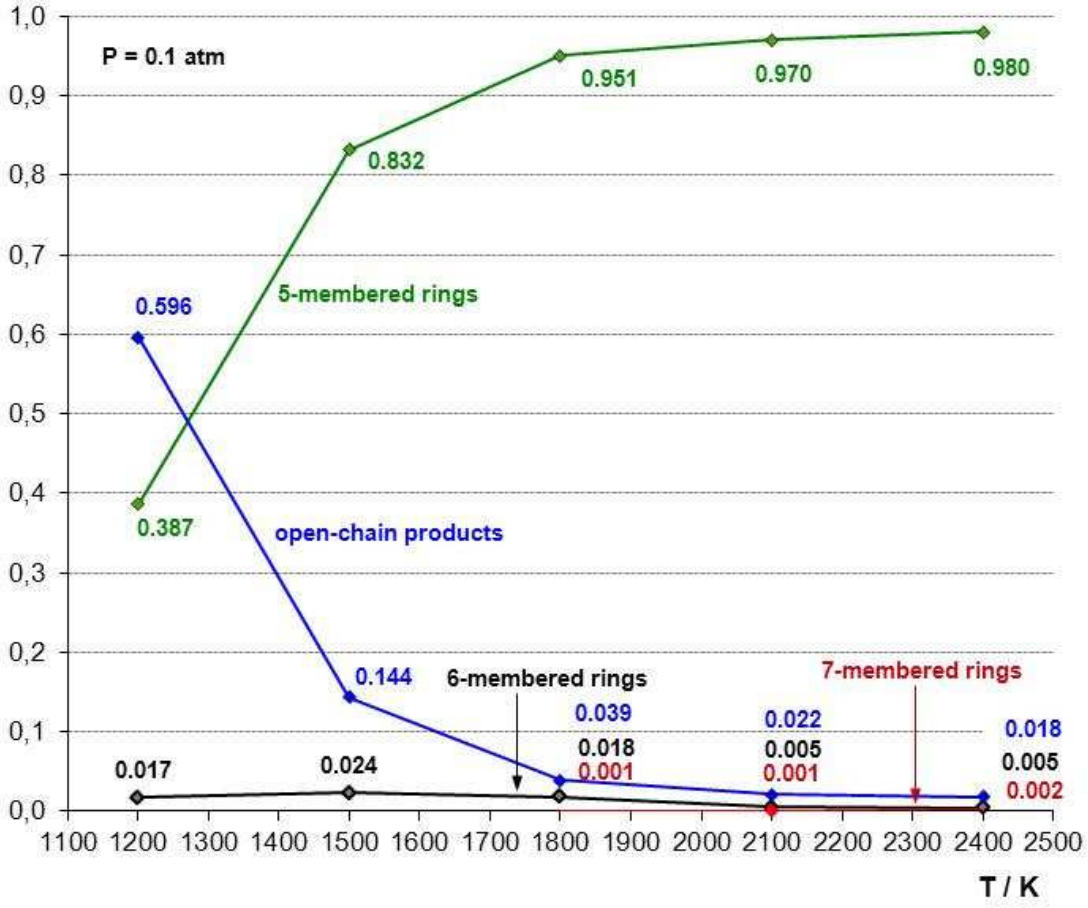

c

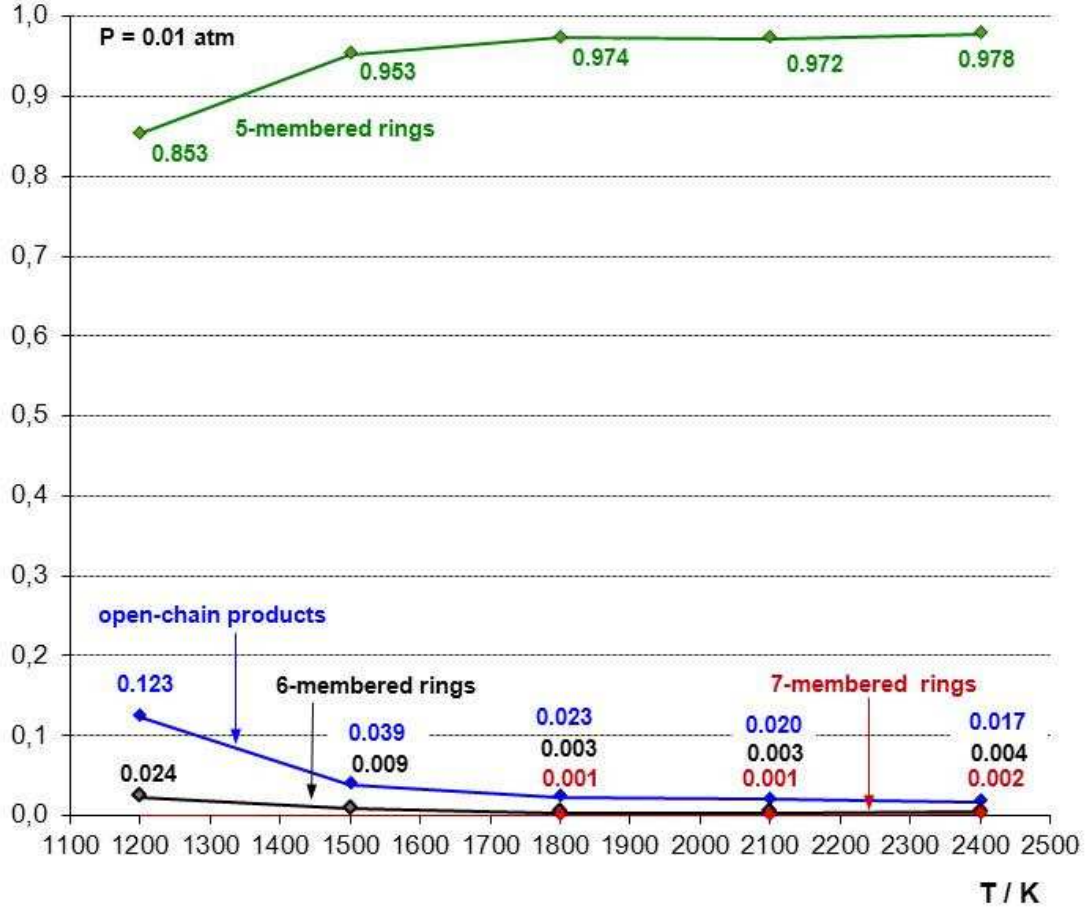

d

Figure 4. Net product reaction yields, at P = 30 atm (a), 1 atm (b), 0.1 atm (c), and 0.01 atm (d).

At P = 0.1 atm (Figure 4c), the crossing point of the yield lines for the 5-rings/open-chains slides further to the left, to about 1250 K. Open-chain products dominate at T = 1200 K, but their yield drops significantly as T increases, falling already to 14% at T = 1500 K, down to 4% and then 0.5% at higher temperatures. By contrast, 5-rings begin to dominate beyond 1300 K, up to 95% (1800 K) and 97% (2100 K). Though 6-rings are again the next contributors, they exhibit a modest 2.4 around 1500 K.

Finally, at P=0.01 atm, the 5-rings/open-chains crossing of the yield lines is no longer present in the plot, due to the T range considered. Open-chain products tend to desappear altogether, and 5-rings clearly dominate over the whole T range (85-97%), though an almost imperceptible declension at high T values appears (Figure 4d). Though 6-rings as a group are again the third contributors, they present very low yields, with a modest 2.4-1% in the range 1200-1400 K.

If we make cuts for some T while considering all four plots, we notice that, by varying P, a declension of open chain product yield with declining pressure is apparent (e.g. 97-49-14-4% at T=1500 K). It is opposed to a more or less pronounced rising yield of 5-rings (3-49-83-95% at T=1500 K). As regards 6-rings, they always form in modest quantities, showing a maximum (2.4-2.7% high) which moves to lower temperatures as pressure is lowered. Minuscule quantities of 7-rings, of the order of 0.2%, form at all pressures at the highest T values. In summary, the effect of pressure (thermalization) is evident from Figure 4, since it offers sort of an animation made by four frames, in which the lines corresponding to the various classes of products move to the left in going from 4a to 4d. Open-chain products are favored by higher pressure and lower temperature: this is understandable in terms of their principal contributors, the initial adducts, and their inclination to proceed reacting further, which is promoted by lower P and higher T conditions. The reverse is true for 5-rings. At intermediate pressures, the dependence from T is more pronounced, while at the lowest pressure temperature is not as important. The T dependence of the yields (slope of their lines) is more pronounced close to crossing region of the yield lines. Since the crossing point slides to the left (lower T) upon P lowering, the line slopes become less pronounced at the lowest P values considered.

We can provide now some limited information, just for some temperatures, about the contribution of single stable intermediates within each class of products. At P = 30 atm, 5-rings become prominent beyond 2200 K, and the fulvenallene + H couple (62) is by far their most important representative: at T = 2400 K, for instance, it represents 70% of the 5-ring share. 6-Rings are only at most 2.7%, out of which benzyl (29), as expected on the basis of its ΔE_{ZPVE}

value, contributes with a 2.5%, followed by 43 (0.2%). At P = 1 atm and T = 1800 K, fulvenallene + H (62) dominates more definitely among 5-rings (77.8% out of a total of 77.9%). As regards 6-rings, benzyl 29 contributes with a 2.4% out of a total of 2.5%, accompanied by the intermediate 43 (0.1%). At P = 0.1 atm and T = 1500 K, 62 represents again 83.1% out of a total of 83.2% of 5-rings. Among 6-rings, with a total of 2.4%, 29 is present with 2.3% yield and 43 with 0.1%. Finally, at P = 0.01 atm and T = 1200 K, 62 represents almost the totality of 5-rings (85.3%), while, among 6-rings, 29 is present with a 2.3% out of a total of 2.4%.

Of the three very stable intermediates (deep energy wells) on which the first part of our study drew our attention, only the benzyl radical is still present with modest yields, because the other wells are depleted by irreversible fragmentation steps.

Plots of rate constant estimates for the formation of the main individual products and classes of products (5-, 6-, and 7-rings), are displayed, as a function of temperature, in the Supporting Information.

Table 2. Rate parameters for overall reactions of 5, 6 and 7-rings formations [a]

	5-rings[b]			6-rings[c]			7-rings[d]		
P [e]	B	n	E_a	B	n	E_a	B	n	E_a
30	1.80×10^{32}	-12.30	52.27	2.43×10^{67}	-22.14	87.59	1.43×10^{-43}	7.48	-7.40
1	5.46×10^{47}	-16.70	60.60	1.88×10^{100}	-31.77	101.54	1.01×10^{-14}	-0.14	24.18
0.1	1.85×10^{29}	-11.69	42.94	9.80×10^{68}	-23.55	67.80	2.29×10^{-3}	-3.28	32.80
0.01	1.56×10^{-4}	-2.55	15.39	1.76×10^{-30}	3.52	-16.40	5.17×10^{-21}	1.65	18.90

[a] $k(T) = B\,T^n \exp(-E_a/RT)$. B in $cm^3\ mol^{-1}\ s^{-1}$, E_a in kcal mol^{-1}. [b] almost exclusively **62**. [c] mainly **29**, **30**, and **43**. [d] mainly **14**, **23**, and **27**. [e] Pressure in atm.

Rate constants for the 5-rings formation from propargyl + but-1-ene-3-yne (Table 2) is in the order of 10^{-14}-10^{-15} $molec^{-1}\ cm^3\ s^{-1}$ (in the range of pressures 0.01-30 atm, and temperatures 1200-2100 K). These k(T) can be compared with those reported by da Silva e Trevitt for the reaction propargyl radical + butadiyne, similar to that studied here.[72] They report rate constants for the formation of 5-membered rings of about 10^{-14}-10^{-16} $molec^{-1}\ cm^3\ s^{-1}$ (T = 1100-2100 K), a range of values close to our results. 6-Ring formation is 1-2 orders of magnitude slower: 10^{-15}-10^{-16} $molec^{-1}\ cm^3\ s^{-1}$ in the range 1200-1800 K. Rate constants for 7-rings formation are at least 3 orders of magnitude smaller than for 5-rings: 10^{-17}-10^{-19} $molec^{-1}\ cm^3\ s^{-1}$.

4. Conclusions

The present study has considered two reacting molecules, the propargyl radical and but-1-ene-3-yne (vinylacetylene), which have been reported to reach, both, significant molar fractions in flames, of the order of $x = 10^{-3}$.

First, the DFT study of the potential energy hypersurface focuses on reaction pathways, apt to form initial 5-, 6-, and 7-membered carbon rings under combustion conditions. They can be regarded as precursors of larger polycyclic systems (PAHs, soot platelets) known to be typically present in combustion processes. Several pathways, leading to both aromatic and non-aromatic ring structures, result more or less promising when ΔE_{ZPVE} is considered. Vinylcyclopentadienyl, benzyl, and tropyl radicals are the stablest intermediates obtained (-79, -84, and -101 kcal mol^{-1} below the reagents, respectively).

Then, the subsequent RRKM part of this study, carried out at different temperatures, shows that different scenarios emerge, depending on pressure. Figures 4a to 4d share some common features.

(1) One is that the yield in **open-chain structures** (mainly represented by the initial adducts), declines with rising T, and almost mirrors, at all pressures, the trend exhibited by **5-rings**, whose yield grows up with T. These two are the main product classes. An evident feature is that the crossing point of the two yield lines apparently moves towards lower T values as P declines. Proceeding from P = 30, to 1, and then to 0.1 atm, the crossing moves from T = 2200 to 1500 K, then to 1250 K. At P=0.01 atm, it disappears from the plots, having presumably moved far to the left, at temperatures not considered in this study. Higher P and lower T favor open-chain products. The main contributors to this class are the initial adducts, which makes this feature understandable in terms of they being inclined, or not, to proceed any further (their evolution is promoted by lower P and higher T conditions). For 5-rings, in particular fulvenallene as end product, the opposite is valid.

At the higher pressures (30 to 0.1 atm), the dependence of the two yield lines of open-chain structures and 5-rings from T is more evident, while T is not as important at the lowest P considered here (0.01 atm). The reason behind this feature is that the slope of the yield lines is more pronounced close to crossing region, and this moves to lower T values as P drops.

(2) Another constant trait is that **6-rings** are the third contributor (mainly represented by the benzyl radical), though they are present at most only with a modest 2.7%. The yield in 6-rings plotted as a function of T presents a flat maximum zone. The maximum zone location varies with the pressure: at higher P, the maximum is located at higher T, at lower P it moves to lower T.

In conclusion, it appears that the propargyl radical plus but-1-ene-3-yne reacting system might offer an interesting opportunity for the formation of 5-membered cyclic carbon systems, in particular at lower pressure and higher temperature. In particular, the fulvenallene system, already indicated as particularly stable by Cavallotti, Derudi, and Rota,[61] as well as by da Silva, Cole, and Bozzelli[62,63] (as the outcome of benzyl decomposition), is favored by this reaction too. By contrast, 6-ring formation appears to be a minor channel, probably because the benzyl well, though very deep, can be reached only in a more indirect way, compared to fulvenallene (Scheme 2). In fact, vinylcyclopentadienyl is attained very soon and can transform to fulvenallene in a single, irreversible, hydrogen loss step.

5. Appendix. Method validation.

Thermodynamic and kinetic data were used to validate the computational level chosen for this study [DFT(M06-2X)/CBS//DFT(M06-2X)/cc-pV*TZ* for energies and geometries; DFT(M06-2X)/cc-pV*TZ* for the assessment of the thermochemistry]. Five reactions were first considered, and a comparison between the relevant experimental and computational reaction enthalpies drawn (Table 3).

Table 3. Experimental vs. theoretically assessed reaction enthalpies for cases 1-5.

	ΔH /kcal mol^{-1}		
	experimental	theoretical	
Reaction		DFT(M06-2X)[g]	CCSD(T)[h]
1	-101.9 ± 1.5 [a,b,d]	-103.6	-102.6
2	-142.20 ± 1.43 [a,c]	-148.7	-149.3
3	-142.77 ± 0.22 [f,c]	-147.7	-145.6
4	-280 ± 1 [f,d]	-289.4	-282.5
5	-88.78 ± 1.02[a,e,f]	-91.3	-92.0
	Mean Signed Error	*-5.01*	*-3.27*
	Mean Unsigned Error	*5.01*	*3.27*

[a]propargyl radical: ref [123]; [b] but-1-ene-3-yne: ref [124]; [c] benzene: ref [125];
[d]benzyl radical: ref 123; [e]propyne: ref [126]; [f]hydrogen atom and ethyne: ref [127]; [g]geometry optimization and thermochemistry at this level of theory;
[h]single-point energy computation at CCSD(T)/CBS level on M06-2X/cc-pV*TZ* geometry, plus M06-2X/cc-pV*TZ* thermochemistry.

Reaction #1 is part of the present study: the formation of the benzyl radical from propargyl and but-1-ene-3-yne (see Scheme 1). Reaction #2 is the formation of benzene starting with two propargyl radicals (see the studies reported in the Introduction). Reaction #3 is ethyne trimerization to give benzene.[128,129,130,131] Reaction #4 sees seven ethyne molecules put into relation with two benzyl radicals: it is not to be considered as a real reaction, yet it allows a "reaction" enthalpy comparison. Reaction #5 is the radical coupling of propargyl with atomic hydrogen, to get propyne.

Then, the rate constants for the propargyl radical + ethyne reaction were calculated at DFT(M06-2X)/CBS level by using TST theory, at four different temperatures, and compared to experimental data.[132] Calculated rate constants show a very good agreement with the experimental rate constants, as reported in Table 4.

Table 4. Experimental vs. theoretically assessed rate constants for the propargyl radical + ethyne reaction.

	k / molec^{-1} cm^3 s^{-1}	
T /K	experiment	DFT(M06-2X)
800	7.25 x 10^{-16}	2.97 x 10^{-16}
900	1.46 x 10^{-15}	9.21 x 10^{-16}
1000	2.55 x 10^{-15}	2.43 x 10^{-15}
1100	4.03 x 10^{-15}	5.13 x 10^{-15}

Acknowledgments. This work was conducted in the frame of EC FP6 NoE ACCENT and ACCENT–PLUS projects (Atmospheric Composition Change, the European NeTwork of Excellence). Financial support has been provided by the Italian MIUR, within the *Programma di Ricerca Scientifica di Rilevante Interesse Nazionale* "Experimental and theoretical studies of the gas phase processes of fundamental and atmospheric interest" (PRIN 2009, D.M. 19 marzo 2010 n. 51 - prot. 2009SLKFEX_005).

Supporting Information includes: Arrhenius plots of the rate constants for the main products, optimum geometries (cartesian coordinates), energies, vibrational frequencies for reagents, intermediates, and transition structures. This information is available free of charge via the Internet at http://pubs.acs.org.

References

[1] See for instance: Ivleva, N. P.; Messerer, A.; Yang, X.; Niessner, R.; Pöschl, U. Microspectroscopic Analysis of Changes in the Chemical Structure and Reactivity of Soot in a Diesel Exhaust After treatment Model System *Environ. Sci. Technol*. **2007**, *41*, 3702-3707.

[2] Möller, J.-O.; Su, D. S.; Jentoft, R. E.; Wild, U.; Schlögl, R. Diesel Engine Exhaust Emission: Oxidative Behavior and Microstructure of Black Smoke Soot Particulate *Environ. Sci. Technol*., **2006**, *40*, 1231-1236.

[3] Cooke, W. F.; Wilson, J. J. N A Global Black Carbon Aerosol Model. *J. Geophys. Res.* **1996**, *101*, 19395-19409.

[4] Liousse, C.; Penner, J. E.; Chuang, C.; Walton, J. J.; Eddleman, H.; Cachier, H. A Global Three-Dimensional Model Study of Carbonaceous Aerosols *J. Geophys. Res.* **1996**, *101*, 19411-19432.

[5] Wilson, E. H.; Atreya, S. K. Chemical Sources of Haze Formation in Titan's Atmosphere. *Planet. Space Sci.* **2003**, *51*, 1017-1033.

[6] Cherchneff, I.; Barker, J. R.; Tielens, A. G. G. M. Polycyclic Aromatic Hydrocarbon Formation in Carbon-Rich Stellar Envelope *Astrophys. J.* **1991**, *377*, 541-552.

[7] Cernicaro, J.; Heras, A. M.; Pardo, J. R.; Tielens, A. G. G. M.; Guélin, M.; Dartois, E.; Neri, R.; Waters, L. B. F. M. Methylpolyynes and Small Hydrocarbons in CRL 618 *Astrophys. J.,* **2001**, *546*, L127-L130.

[8] Cernicaro, J. The Polymerization of Acetylene, Hydrogen Cyanide, and Carbon Chains in the Neutral Layers of Carbon-rich Proto-planetary Nebulae *Astrophys. J.,* **2004**, *608*, L41-L44.

[9] Cherchneff, I. The Formation of Polycyclic Aromatic Hydrocarbons in Evolved Circumstellar Environments, in: *PAHs and the Universe*, Joblin, C. & Tielens, A. G. G. M. (Eds.), EAS Publications Series, Vol. 46, 2010.

[10] Allamandola, L. J.; Tielens, A. G. G. M.; Barker, J. R. Interstellar Polycyclic Aromatic Hydrocarbons: The Infrared Emission Bands, the Excitation/Emission Mechanism, and the Astrophysical Implications *Astrophys. J. Suppl. Series* **1989**, *71*, 733-775.

[11] Zhou, L.; Zheng, W.; Kaiser, R. I.; Landera, A.; Mebel, A. M.; Liang, M.-C. Cosmic-ray-mediated Formation of Benzene on the Surface of Saturn's Moon Titan *Astrophys. J.* **2010**, *718*, 1243-1251.

[12] See for instance: Yang, X.; Dou, X.; Zhi, L.; Räder, H. J.; Müllen, K. Two-Dimensional Graphene Nanoribbons *J. Am. Chem. Soc.* **2008**, *130*, 4216-4217, and the three references which follow.

[13] Müller, S.; Müllen, K. Expanding Benzene to Giant Graphenes: Towards Molecular Devices *Phil. Trans. R. Soc. A,* **2007**, *365*, 1453-1472.

[14] Wu, J.; Pisula, W.; Müllen, K. Graphenes as Potential Material for Electronics *Chem. Rev.,* **2007**, *107*, 718-747.

[15] Simpson, C. D.; Brand, J. D.; Berresheim, A. J.; Przybilla, L.; Räder, H. J.; Müllen, K. Synthesis of a Giant 222 Carbon Graphite Sheet *Chem. Eur. J.* **2002**, *8*, 1424-1429.

[16] Wie, D.; Liu Y. Controllable Synthesis of Graphene and its Applications *Adv. Mater.* **2010**, *22*, 3225-3241.

[17] Yu, D. S.; Dai, L. M. Self-Assembled Graphene/Carbon Nanotube Hybrid Films for Supercapacitors *J. Phys. Chem. Lett.* **2010**, *1*, 467-470.

[18] Wang, Y.; Shi, Z. Q.; Huang, Y.; Ma, Y. F.; Wang, C. Y.; Chen, M. M.; Chen, Y. S. Supercapacitor Devices Based on Graphene Materials *J. Phys. Chem. C* **2009**, *113*, 13103-13107.

[19] Al-Mashat, L.; Shin, K.; Kalantar-Zadeh, K.; Plessis, J. D.; Han, S. H.; Kojima, R. W.; Kaner, R. B.; Li, D.; Gou, X. L.; Ippolito, S. J.; Wlodarski, W. Graphene/Polyaniline Nanocomposite for Hydrogen Sensing *J. Phys. Chem. C* **2010**, *114*, 16168-16173.

[20] Hong, W. J.; Bai, H.; Xu, Y. X.; Yao, Z. Y.; Gu, Z. Z.; Shi, G. Q. Preparation of Gold Nanoparticle/Graphene Composites with Controlled Weight Contents and Their Application in Biosensors *J. Phys. Chem. C* **2010**, *114*, 1822-1826.

[21] Areshkin, D. A.; White, C.T. Building Blocks for Integrated Graphene Circuits *Nano Lett.,* **2007**, *7*, 3253-3259.

[22] Finlayson-Pitts, B. J.; Pitts, J. N., Jr., *Chemistry of the Upper and Lower Atmosphere*; Academic Press, New York, 2000, ch. 10. See, in particular, Figures 10.2 and 10.3.

[23] See for instance: Böhm, H.; Jander, H. PAH Formation in Acetylene–Benzene Pyrolysis *Phys. Chem. Chem. Phys.* **1999**, *1*, 3775-3781, and the four references which follow.

[24] Ledesma, E. B.; Kalish, M. A.; Nelson, P. F.; Wornat, M. J.; Mackie, J. C. Formation and fate of PAH During the Pyrolysis and Fuel-Rich Combustion of Coal Primary Tar *Fuel* **2000**, 79, 1801-1814.

[25] Naydenova, I.; Vlasov, P. A.; Warnatz, J. Development of Kinetic Modelling of Soot Formation during Shock Tube Pyrolysis and Oxidation of Hydrocarbons of Different Types *Proc. Eur. Comb. Meeting* **2005**, 1-4.

[26] Jäger, C.; Huisken, F.; Mutschke, H.; Llamas-Jansa, I.; Henning, Th. Formation of Polycyclic Aromatic Hydrocarbons and Carbonaceous Solids in Gas-Phase Condensation Experiments *Astrophys. J.* **2009**, *696*, 706-712.

[27] Jäger, C.; Mutschke, H.; Huisken, F.; Krasnokutski, S.; Staicu, A.; Henning, Th.; Poppitz, W.; Voicu, I. Identification and Spectral Properties of Polycyclic Aromatic Hydrocarbons in Carbonaceous Soot Produced by Laser Pyrolysis *Astrophys. J. Suppl.* **2006**, *166*, 557-566.

[28] Siegmann, Sattler, and Siegmann, on the basis of their experimental results (relevant to atmospheric-pressure flames), put forward the hypothesis that soot synthesis can even precede PAH synthesis: Siegmann, K.; Sattler, K.; Siegmann, H. C. Clustering at High Temperatures: Carbon Formation in Combustion *J. Electron Spectr.* 2002, **126**, 191-202.

[29] Homann, K.-H. Fullerenes and Soot Formation - New Pathways to Large Particles in Flames *Angew. Chem. Int. Ed.* **1998**, *37*, 2434-2451.

[30] Indarto, A.; Giordana, A.; Ghigo, G.; Maranzana, A.; Tonachini, G. Polycyclic Aromatic Hydrocarbon Formation Mechanism in the "Particle Phase". A Theoretical Study *Phys. Chem. Chem. Phys*. **2010**, *12*, 9429-9440.

[31] Giordana, A.; Maranzana, A.; Tonachini, G. Theoretical Investigation of Soot Nanoparticle Inception via Polycyclic Aromatic Hydrocarbon Coagulation (Condensation): Energetic, Structural, and Electronic Features *J. Phys. Chem. C* **2011**, *115*, 1732-1739.

[32] Giordana, A.; Maranzana, A.; Tonachini, G. Nanoparticle Molecular Inception from Radical Addition and van der Waals Coagulation of Polycyclic Aromatic Hydrocarbon-Based Systems. A Theoretical Study *J. Phys. Chem. C* **2011**, *115*, 17237-17251.

[33] Richter, H.; Howard, J. B. Formation of Polycyclic Aromatic Hydrocarbons and Their Growth to Soot -A Review of Chemical Reaction Pathways *Prog. En. Combust. Sci.* **2000**, *26*, 565-608, and references therein.

[34] Frenklach, M. Reaction Mechanism of Soot Formation in Flames *Phys. Chem. Chem. Phys.* **2002**, *4*, 2028-2037. In particular, section 2.1.

[35] Bittner, J. D.; Howard, J. B. Composition Profiles and Reaction Mechanisms in a Near-sooting Premixed Benzene/Oxygen/Argon Flame *Proc. Combust. Inst.* **1981**, *18*, 1105-1116.

[36] Cole, J. A.; Bittner, J. D.; Longwell, J. P.; Howard, J. B. Formation Mechanisms of Aromatic Compounds in Aliphatic Flames *Combust. Flame* **1984**, *56*, 51-70.

[37] Frenklach, M.; Clary, D. W., Yuan, T., Gardiner, Jr. W. C., Stein S. E. Mechanism of Soot Formation in Acetylene-Oxygen Mixtures *Combust. Sci. & Technol.* **1986**, *50*, 79-115.

[38] Richter, H.; Howard, J. B. Formation and Consumption of Single-Ring Aromatic Hydrocarbons and their Precursors in Premixed Acetylene, Ethylene and Benzene Flames *Phys. Chem*. *Chem*. *Phys.* **2002**, *4*, 2038-2055.

[39] Frenklach, M.; Warnatz, J. Detailed Modeling of PAH Profiles in a Sooting Low-Pressure Acetylene Flame *Comb. Sci. & Tech*. **1987**, *51*, 265–283.

[40] Westmoreland, P. R.; Dean, A. M.; Howard, J. B.; Longwell, J. P. Forming Benzene in Flames by Chemically Activated Isomerization *J. Phys. Chem*. **1989**, *93*, 8171-8180.

[41] Miller, J. A.; Melius, C. F. Kinetic and Thermodynamic Issues in the Formation of Aromatic Compounds in Flames of Aliphatic Fuels *Combust. Flame*, **1992**, *91*, 21-39.

[42] Melius, C. F.; Miller, J.; Evleth E. M. Unimolecular Reaction Mecvhanisms Involving C_3H_4, C_4H_4, and C_6H_6 Hydrocarbon Species *Proc. Combust. Inst.*, **1992**, *24*, 621-628.

[43] Alkemade, U.; Homann, K.-H. Formation of C_6H_6 Isomers by Recombination of Propynyl in the System Sodium Vapor Propynylhalide *Zeitschrift Fur Physikalische Chemie Neue Folge* **1989**, *161*, 19-34.

[44] Marinov, N. M.; Castaldi, M. J.; Melius, C. F., Tsang W. Aromatic and Polycyclic Aromatic Hydrocarbon Formation in a Premixed Propane Flame *Combust. Sci. Technol*. **1997**, *128*, 295-342.

[45] Stein, S. E.; Walker, J. A.; Suryan M. M.; Fahr A. A New Path to Benzene in Flames *23rd Intl. Symp. Combust*., **1990**, 85-90.

[46] Miller, J. A.; Klippenstein, S. J. The Recombination of Propargyl Radicals and Other Reactions on a C_6H_6 Potential *J. Phys. Chem. A* **2003**, *107*, 7783-7799.

[47] Atkinson, D. B.; Hudgens, J. W. Rate Coefficients for the Propargyl Radical Self-Reaction and Oxygen Addition Reaction Measured Using Ultraviolet Cavity Ring-down Spectroscopy *J. Phys. Chem. A,* **1999**, *103*, 4242-4252.

[48] Rasmussen, C. L.; Skjøth-Rasmussen, M. S.; Jensen, A. D.; Glarborg, P. Propargyl Recombination: Estimation of the High Temperature, Low Pressure Rate Constant from Flame Measurements *Proc. Combust. Inst.,* **2005**, *30*, 1023–1031.

[49] Hoyermann, K.; Mauss, F.; Zeuch, Th. A Detailed Chemical Reaction Mechanism for the Oxidation of Hydrocarbons and its Application to the Analysis of Benzene Formation in Fuel-Rich Premixed Laminar Acetylene and Propene Flames *Phys. Chem. Chem. Phys.,* **2004,** *6*, 3824–3835.

[50] Hansen, N.; Kasper, T.; Klippenstein, S. J.; Westmoreland, P. R.; Law, M. E.; Taatjes, C. A.; Kohse-Höinghaus, K.; Wang, J.; Cool, T. A. Initial Steps of Aromatic Ring Formation in a Laminar Premixed Fuel-Rich Cyclopentene Flame *J. Phys. Chem. A* **2007**, *111*, 4081-4092. In this experimental and theoretical paper the mole fraction profiles of several C_5 species, and other known benzene precursors, as C_3H_3, C_3H_5, C_4H_3, and C_4H_5, are determined, as well as the isomeric composition of C_4H_4, C_4H_6, C_4H_8, C_7H_6, and C_7H_8 species. Then, the presence of $C_5H_4CCH_2$, C_5H_5CCH, and cycloheptatriene suggests pathways toward aromatic species. See also the three references which follow.

[51] Hansen, N.; Li, W.; Law, M. E.; Kasper, T.; Westmoreland, P. R.; Yang, B.; Cool, T. A.; Lucassen, A. The Importance of Fuel Dissociation and Propargyl + Allyl Association for the Formation of Benzene in a Fuel-Rich 1-Hexene Flame *Phys. Chem. Chem. Phys.,* **2010**, *12*, 12112–12122.

[52] Hansen, N.; Klippenstein, S. J.; Taatjes, C. A.; Miller, J. A.; Wang, J.; Cool, T. A.; Yang, B.; Yang, R.; Wei, L.; Huang, C.; Wang, J.; Qi, F.; Law, M. E.; Westmoreland, P. R. Identification and Chemistry of C_4H_3 and C_4H_5 Isomers in Fuel-Rich Flames *J. Phys. Chem. A*, **2006**, *110*, 3670-3678.

[53] Hansen, N.; Miller, J. A.; Klippenstein, S. J.; Westmoreland, P. R.; Kohse-Höinghaus, K. Exploring Formation Pathways of Aromatic Compounds in Laboratory-Based Model Flames of Aliphatic Fuels *Comb. Expl. Shock Waves,* **2012***, 48,* 508–515.

[54] Zhang, F.; Jones, B.; Maksyutenko, P.; Kaiser, R. I.; Chin, C.; Kislov, V. V.; Mebel, A. M. Formation of the Phenyl Radical [$C_6H_5(X^2A_1)$] under Single Collision Conditions: A Crossed Molecular Beam and *ab Initio* Study *J. Am. Chem. Soc.* **2010**, *132*, 2672-2683.

[55] Mebel, A. M.; Kislov, V. V. Can the $C_5H_5 + C_5H_5 \rightarrow C_{10}H_{10} \rightarrow C_{10}H_9 + H/C_{10}H_8 + H_2$ Reaction Produce Naphthalene? An Ab Initio/RRKM Study *J. Phys. Chem. A* **2009**, *113*, 9825-9833.

[56] Mebel, A. M.; Kislov, V. V.; Kaiser, R. I. Photoinduced Mechanism of Formation and Growth of Polycyclic Aromatic Hydrocarbons in Low-Temperature Environments via Successive Ethynyl Radical Additions *J. Am. Chem. Soc.* **2008**, *130*, 13618-13629.

[57] Kaiser, R. I.; Parker, D. S. N.; Zhang, F.; Landera, A.; Kislov, V. V.; Mebel, A. M. PAH Formation under Single Collision Conditions: Reaction of Phenyl Radical and 1,3-Butadiene to Form 1,4-Dihydronaphthalene *J. Phys. Chem. A* **2012**, *116*, 4248−4258.

[58] Kislov, V. V.; Mebel, A. M. Ab Initio G3-type/Statistical Theory Study of the Formation of Indene in Combustion Flames. I. Pathways Involving Benzene and Phenyl Radical *J. Phys. Chem. A* **2007**, *111*, 3922-3931.

[59] Landera, A.; Mebel, A. M.; Kaiser, R. I. Theoretical Study of the Reaction Mechanism of Ethynyl Radical with Benzene and Related Reactions on the C8H7 Potential Energy Surface *Chem. Phys. Lett*., **2008**, *459*, 54–59**.**

[60] Vereecken, L.; Peeters, J.; Bettinger, H. F.; Kaiser, R. I.; Schleyer, P. v. R.; Schaefer, H. F. III Reaction of Phenyl Radicals with Propyne *J. Am. Chem. Soc.* **2002**, *124*, 2781-2789.

[61] Cavallotti, C.; Derudi, M.; Rota, R. On the Mechanism of Decomposition of the Benzyl Radical *Proc. Combust. Inst.* **2009**, *32*, 115–121.

[62] da Silva, G.; Cole, J. A.; Bozzelli, J. W. Kinetics of the Cyclopentadienyl + Acetylene, Fulvenallene + H, and 1-Ethynylcyclopentadiene + H Reactions *J. Phys. Chem. A* **2010,** *114,* 2275–2283.

[63] da Silva, G.; Cole, J. A.; Bozzelli, J. W. Thermal Decomposition of the Benzyl Radical to Fulvenallene (C_7H_6) + H *J. Phys. Chem. A* **2009,** *113,* 6111–6120.

[64] Saha, B.; Irle, S.; Morokuma, K. Formation Mechanism of Polycyclic Aromatic Hydrocarbons in Benzene Combustion: Quantum Chemical Molecular Dynamics Simulations *J. Chem. Phys.* **2010**, *132*, 224303 (1-11).

[65] Indarto, A.; Giordana, A.; Ghigo, G.; Tonachini, G. Formation of PAHs and Soot Platelets: Multiconfiguration Theoretical Study of the Key Step in the Ring Closure-Radical Breeding Polyyne-Based Mechanism *J. Phys. Org. Chem.* **2010**, *23*, 400-410.

[66] Krestinin, A.V. Detailed Modeling of Soot Formation in Hydrocarbon Pyrolysis *Combust. Flame* **2000**, *121*, 513-524.

[67] Krestinin, A.V. Formation of Soot Particles as a Process Involving Chemical Condens-ation of Polyynes *Chem. Phys. Rep.* **1998**, *17*, 1441-1461.

[68] Krestinin, A.V. On the Mechanism of Soot Formation from Acetylene *Chem. Phys. Rep.* **1994**, *13*, 191-210.

[69] Homann, K.-H.; Wagner, H.G. Some New Aspects of the Mechanism of Carbon Formation in Premixed Flames *Intl. Symp. Combust*., **1967**, *11*, 371-379.

[70] Kniazev, V. D.; Slagle, I. R. Kinetics of the Reaction between Propargyl Radical and Acetylene *J. Phys. Chem. A* **2002**, *106*, 5613-5617.

[71] Moskaleva, L. V.; Lin, M. C. Unimolecular Isomerization/Decomposition of Cyclopentadienyl and Related Bimolecular Reverse Process: Ab Initio MO/Statistical Theory Study *J. Comput. Chem.* **2000**, *21*, 415-425.

[72] da Silva, G.; Trevitt, A. Chemically Activated Reactions on the C_7H_5 Energy Surface: Propargyl + Diacetylene, *i*-C_5H_3 + Acetylene, and *n*-C_5H_3 + Acetylene *Phys. Chem. Chem. Phys.* **2011**, *13*, 8940-8952.

[73] Maranzana, A.; Indarto, A.; Ghigo, G.; Tonachini, G. Assessing First Ring Formation in Polycyclic Aromatic Hydrocarbon and Soot Combustive Formation Started by the Radical Addition of Propargyl to Butadiyne. A RRKM/DFT Study *Combust. Flame*, **2013**, *160*, 2333-2342.

[74] Propargylic radicals are seen as interesting reactants in organic synthesis. However they are found to react rather sluggishly with alkenes, and activated alkenes are needed to carry out addition reactions conveniently. Methods to generate them (or equivalent synthons) and have them reacted with C=C bonds have been consequently devised. See the two references that follow.

[75] Boutillier, P.; Zard, S. Z. Synthetic Equivalents of Alkynyl and Propargyl Radicals *Chem. Commun*. **2001**, 1304-1305.

[76] Denieul, M.-P.; Quiclet-Sire, B.; Zard, S. Z. A synthetically useful source of propargyl radicals *Tetrah.Lett.* **1996**, *37*, 5495-5498.

[77] Maximum mole fractions reported are:
ref. 78: x = 1.6×10^{-4} (but-1-yne-3-ene) and 2.1×10^{-3} (propargyl)
ref. 79: x = 2.1×10^{-3} (but-1-yne-3-ene) and 2.4×10^{-3} (propargyl)
ref. 80: x = 7.7×10^{-4} (but-1-yne-3-ene) and 2.8×10^{-3} (propargyl)
ref. 81: x = 1.38×10^{-3} (but-1-yne-3-ene) and 3.10×10^{-3} (propargyl)

[78] Li, Y.; Zhang, L.; Tian, Z.; Yuan, T.; Zhang, K.; Yang, B.; Qi Fei Investigation of the Rich Premixed Laminar Acetylene/Oxygen/Argon Flame: Comprehensive Flame Structure and Special Concerns of Polyynes *Proc. Combust. Inst.* **2009**, *32*, 1293-1300.

[79] Yang, B.; Li, Y.; Wei, L.; Huang, C.; Wang, J.; Tian, Z.; Yang, R.; Sheng, L.; Zhang, Y.; Qi F. An Experimental Study of the Premixed Benzene/Oxygen/Argon Flame with Tunable Synchrotron Photoionization *Proc. Combust. Inst.* **2007**, *31*, 555-563.

[80] Li, Y.; Zhang, L.; Tian, Z.; Yuan, T.; Wang, J.; Yang, B.; Qi, F. Experimental Study of a Fuel-Rich Premixed Toluene Flame at Low Pressure *Energy & Fuels* **2009,** *23,* 1473-1485 (toluene flame).

[81] Li, Y.; Huang, C.; Wei, L.; Yang, B.; Wang, J.; Tian, Z.; Zhang, T.; Yang, R.; Sheng, L.; Qi, F. An Experimental Study of Rich Premixed Gasoline/O_2/Ar Flame with Tunable Synchrotron Vacuum Ultraviolet Photoionization *Energy & Fuels* **2007,** *21,* 1931-1941.

[82] Wang, J.; Struckmeier, U.; Yang, B.; Cool, T. A.; Osswald, P.; Kohse-Höinghaus, K.; Kasper, T.; Hansen, N.; Westmoreland, P. R. Isomer-Specific Influences on the Composition of Reaction Intermediates in Dimethyl Ether/Propene and Ethanol/Propene Flame *J. Phys. Chem. A,* **2008**, *112*, 9255–9265.

[83] Defoeux, F.; Dias, V.; Renard, C.; Van Tiggelen, P. J.; Vandooren, J. Experimental Investigation of the Structure of a Sooting Premixed Benzene/Oxygen/Argon Flame Burning at Low Pressure *Proc. Combust. Inst.,* **2005**, *30*, 1407–1415.

[84] Pople, J. A.; Gill, P. M. W.; Johnson, B. G. Kohn—Sham Density-Functional Theory within a Finite Basis Set *Chem. Phys. Lett.* **1992**, *199*, 557-560.

[85] Schlegel, H. B.; in *Computational Theoretical Organic Chemistry*, ed. Csizsmadia, I. G.; Daudel, R., Reidel Publishing Co., Dordrecht, The Netherlands, 1981, pp. 129-159.

[86] Schlegel, H. B. An Efficient Algorithm for Calculating Ab Initio Energy Gradients Using s,p Cartesian Gaussians *J. Chem. Phys.* **1982**, *77*, 3676-3681.

[87] Schlegel, H. B.; Binkley, J. S.; Pople, J. A. First and Second Derivatives of Two Electron Integrals over Cartesian Gaussians Using Rys Polynomials *J. Chem. Phys.* **1984**, *80*, 1976-1981.

[88] Schlegel, H. B. Optimization of Equilibrium Geometries and Transition Structures *J. Comput. Chem*. **1982**, *3*, 214-218.

[89] Parr, R. G.; Yang, W. *Density Functional Theory of Atoms and Molecules*, Oxford University Press: New York, 1989, ch. 3.

[90] Zhao, Y.; Truhlar, D. G. The M06 Suite of Density Functionals for Main Group Thermochemistry, Thermochemical Kinetics, Noncovalent Interactions, Excited States, and Transition Elements: Two New Functionals and Systematic Testing of four M06-class functionals and 12 Other Functionals *Theor. Chem. Acc*., **2008**, *120*, 215-241.

[91] Zhao, Y.; Truhlar, D. G. Density Functionals with Broad Applicability in Chemistry *Acc. Chem. Res.*, **2008**, *41*, 157-167.

[92] Zhao, Y.; Truhlar, D. G. How Well Can New-Generation Density Functionals Describe the Energetics of Bond-Dissociation Reactions Producing Radicals? *J. Phys. Chem. A*, **2008**, *112*, 1095-1099.

[93] Zhao, Y.; Truhlar, D. G. Exploring the Limit of Accuracy of the Global Hybrid Meta Density Functional for Main-Group Thermochemistry, Kinetics, and Noncovalent Interactions *J. Chem. Theory & Comput*., **2008**, *4*, 1849-1868.

[94] Kendall, R. A.; Dunning, T. H., Jr.; Harrison, R. J. Electron Affinities of the First-Row Atoms Revisited. Systematic Basis Sets and Wave Functions *J. Chem. Phys.* **1992**, *96*, 6796-6806.

[95] Woon, D. E.; Dunning, T. H., Jr. Gaussian Basis Sets for Use in Correlated Molecular Calculations. III. The atoms aluminum through argon *J. Chem. Phys.* **1993**, *98*, 1358-1372.

[96] Halkier, A.; Helgaker, T.; Jørgensen, P.; Klopper, W.; Koch, H.; Olsen, J.; Wilson, A. K. Basis-set Convergence in Correlated Calculations on Ne, N_2, and H_2O *Chem. Phys. Lett.* **1998**, *286*, 243-252.

[97] Gaussian 09, Revision A.02, Frisch, M. J.; Trucks, G. W.; Schlegel, H. B.; Scuseria, G. E.; Robb, M. A.; Cheeseman, J. R.; Scalmani, G.; Barone, V.; Mennucci, B.; Petersson, G. A. et al. Gaussian, Inc., Wallingford CT, 2009.

[98] Holbrook, K.A.; Pilling, M.J.; Robertson, S.H. "Unimolecular reactions". John Wiley & Sons, Chichester, 1996.

[99] Gilbert, R. G.; Smith, S. C. "Theory of unimolecular and recombination reactions". Blackwell Scientific, Oxford, 1990.

[100] Lindemann, F. A. Discussion on "The Radiation Theory of Chemical Action" *Tran. Faraday Soc*. **1922**, *17*, 598-606.

[101] Hinshelwood, C. N. On the Theory of Unimolecular Reactions *Proc. Roy. Soc.* **1927**, *A113*, 230-233.

[102] MultiWell-2012.2 Software, July 2012, designed and maintained by J. R. Barker with contributors Ortiz, N. F.; Preses, J. M.; Lohr, L. L.; Maranzana, A.; Stimac, P. J.; Nguyen, T. L.; Dhilip Kumar T. J., University of Michigan, Ann Arbor, MI; http://aoss.engin.umich.edu/multiwell/.

[103] Barker, J.R. Multiple-Well, Multiple-Path Unimolecular Reaction Systems. I. MultiWell Computer Program Suite *Int. J. Chem. Kinetics* **2001**, *33*, 232-245.

[104] Barker, J.R. Energy Transfer in Master Equation Simulations: A New Approach *Int. J. Chem. Kinetics* **2009**, *41*, 748-763.

[105] Eckart, C. The Penetration of a Potential Barrier by Electrons *Phys. Rev.* **1930**, *35*, 1303-1309.

[106] Da Silva, G.; Moore, E. E.; Bozzelli, J. W. Decomposition of Methylbenzyl Radicals in the Pyrolysis and Oxidation of Xylenes *J. Phys. Chem. A,* **2009,** *113,* 102645–10278.

[107] A larger number of collisions was used in the simulations when it was required by the PPM software (see Ref 82).

[108] Low-pressure flames are oftentimes preferred because of their nearly one dimensional structure and extended reaction zone. See for instance: Hartlieb, A. T.; Atakan, B.; Kohse-Höinghaus, K. Temperature Measurement in Fuel-rich Non-sooting Low-pressure Hydrocarbon Flames *Appl. Phys. B,* **2000**, *70*, 435-445.

[109] Faccinetto, A.; Desgroux, P.; Ziskind, M.; Therssen, E.; Focsa, C. High-Sensitivity Detection Of Polycyclic Aromatic Hydrocarbons Adsorbed onto Soot Particles Using Laser Desorption/Laser Ionization/Time-of-Flight Mass Spectrometry: An Approach to Studying the Soot Inception Process in Low-Pressure Flames *Combust. Flame,* **2011**, *158*, 227-239.

[110] Desgroux, P.; Mercier, X.; Lefort, B.; Lemaire, R.; Therssen, E.; Pauwels, J. F. Soot Volume Fraction Measurement in Low-Pressure Methane Flames by Combining Laser-Induced Incandescence and Cavity Ring-Down Spectroscopy: Effect of Pressure on Soot Formation *Combust. Flame,* **2008**, *155*, 289-301.

[111] Wua, X.; Huang, Z.; Yuan, T.; Zhang, K.; Wei, L. Identification of Combustion Intermediates in a Low-Pressure Premixed Laminar 2,5-Dimethylfuran/Oxygen/Argon Flame with Tunable Synchrotron Photoionization *Combust. Flame,* **2009**, *156*, 1365-1376.

[112] Richter, H.; Granata, S.; Green, W. H.; Howard, J. B. Detailed Modeling of PAH and Soot Formation in a Laminar Premixed Benzene/Oxygen/ Argon Low-Pressure Flame *Proc. Combust. Inst.* **2005**, *30*, 1397-1405.

[113] Richter, H.; Benish, T.G.; Mazyar, O. A.; Green, W. H.; Howard, J. B. Detailed Chemical Kinetics Studies of an NH_3/N_2O/Ar Flame by Laser-Induced Fluorescence, Mass Spectrometry, and Modeling *Proc. Combust. Inst*., **2000**, *28*, 2609-2618.

[114] Rensberger, K. J.; Jeffries, J. B.; Copeland, R. A.; Kohse-Höinghaus, K.; Wise, M. L.; Crosley, D. R. Laser-induced Fluorescence Determination of Temperatures in Low Pressure Flames *Appl. Optics*, **1989**, *28*, 3556-3566.

[115] Yang, B.; Oßwald, P.; Li, Y.; Wang, J.; Wei, L.; Tian, Z.; Qi, F.; Kohse-Höinghaus, K. Identification of Combustion Intermediates in Isomeric Fuel-Rich Premixed Butanol–Oxygen Flames at Low Pressure *Combust. Flame*, **2007**, *148*, 198-209. Tinaut, F. V.; Melgar, A.; Horrillo, A.; Díez de la Rosa, A. Method for Predicting the Performance of an Internal Combustion Engine Fuelled By Producer Gas and Other Low Heating Value Gases *Fuel Process. Tech.,* **2006**, *87*, 135-142.

[116] Pinches S. J.; da Silva, G. On the Separation of Timescales in Chemically Activated Reactions *Int. J. Chem. Kin.,* **2013**, *45,* 387-396.

[117] The tropyl, or cycloheptatrienyl, radical is a Jahn-Teller system, which has been studied both experimentally and theoretically: see the three references that follow. In our computations, one of the two degenerate C_{2v} electronic states is defined, and its energy reported.

[118] Stakhursky, V. L.; Sioutis, I.; Tarczay, G.; Miller, T. A. Computational Investigation of the Jahn-Teller Effect in the Ground and Excited Electronic States of the Tropyl Radical. Part I *J. Chem. Phys.,* **2008**, *128*, 084310 (1-13).

[119] Sioutis, I.; Stakhursky, V. L.; Tarczay, G.; Miller, T. A. Experimental Investigation of the Jahn-Teller Effect in the Ground and Excited Electronic States of the Tropyl Radical. Part II. Vibrational analysis of the $\tilde{A}^2E_3''$-$\tilde{X}^2E_2''$ Electronic Transition *J. Chem. Phys.,* **2008**, *128*, 084311 (1-18).

[120] Lee, E. P. F.; Wright, T. G. The Tropyl Cation (*c*-C_7H_7+) and the Tropyl Radical (*c*-C_7H_7) *J. Phys. Chem. A,* **1998**, *102*, 4007-4013.

[121] Sivaramakrishnan, R.; Su, M.-C.; Michael, J. V. H- and D-atom formation from the pyrolysis of $C_6H_5CH_2Br$ and $C_6H_5CD_2Br$: Implications for high-temperature benzyl decomposition *Proc. Combust. Inst.,* **2011**, *33*, 243–250, and references therein.

[122] The branching ratios were used to weight the entrance channels. The yields calculated for each channel were scaled by the branching ratio.

[123] Tsang, W. Heats of Formation of Organic Free Radicals by Kinetic Methods, in: *Energetics of Organic Free Radicals*, J. A. Martinho Simoes, A. Greenberg, J. F. Liebman (Eds.), Blackie Academic and Professional, London, 1996, p. 22-58.

[124] Roth, W. R.; Adammczak, O.; Breuckmann, R. Resonance Energy Calculation - The MM2ERW Force-field *Chem. Ber*., **1991**, *124*, 2499-2521.

[125] Roux, M. V.; Temprado, M.; Chickos, J. S.; Nagano, Y. Critically Evaluated Thermochemical Properties of Polycyclic Aromatic Hydrocarbons *J. Phys. Chem. Ref. Data*, **2008**, *37*, 1855-1996.

[126] Wagman, D. D.; Kilpatrick, J. E.; Pitzer, K. S.; Rossini, F. D. Heats, Equilibrium Constants, and Free Energies of Formation of the Acetylene Hydrocarbons Through the Pentynes, to 1,500-Degrees K *J. Res. NBS*, **1945**, *35*, 467-496.

[127] Chase, M. W. Jr *NIST-JANAF Thermochemical Tables, Fourth Edition*, *J. Phys. Chem. Ref. Data*, **1998**, Monograph *9*, 1-1951.

[128] Cioslowski, J.; Liu, G.; Moncrieff, D. The Concerted Trimerization of Ethyne to Benzene Revisited *Chem. Phys. Lett.* **2000**, *316*, 536–540, and references therein.

[129] Havenith, R. W. A.; Fowler, P. W.; Jenneskens, L. W.; Steiner, E. Trimerization of Ethyne: Growth and Evolution of Ring Currents in the Formation of the Benzene Ring *J. Phys. Chem. A*, **2003**, *107*, 1867–1871.

[130] Santos, J. C.; Polo, V.; Andrés, J. An Electron Localization Function Study of the Trimerization of Acetylene: Reaction Mechanism and Development of Aromaticity *Chem. Phys. Lett.,* **2005**, *406*, 393–397.

[131] Sakai, S.; Taketa, K. The [2 + 2 + 2] Mechanisms of Trimerization of Three Ethynes and Monosilaethylenes *Theor. Chem. Acc.* **2011**, *130*, 901-907.

[132] Knyazev, V.D.; Slagle, I.R. Kinetics of the Reaction between Propargyl Radical and Acetylene *J. Phys. Chem. A*, **2002**, *106*, 5613-5617.